
Article:
Hussain, F., Khesro, A., Lu, Z. orcid.org/0000-0002-9967-5221 et al. (5 more authors) (2020) Acceptor and donor dopants in potassium sodium niobate based ceramics. Frontiers in Materials, 7. 160.

https://doi.org/10.3389/fmats.2020.00160

---

frontiers in Materials

ORIGINAL RESEARCH
published: 08 July 2020
doi: 10.3389/fmats.2020.00160

Acceptor and Donor Dopants in Potassium Sodium Niobate Based Ceramics

Fayaz Hussain[1,2], Amir Khesro[3], Zhilun Lu[2,4], Nouf Alotaibi[5], Ahmad Azmin Mohamad[6], Ge Wang[2], Dawei Wang[2] and Di Zhou[7]**

[1] Department of Materials Engineering, NED University of Engineering & Technology, Karachi, Pakistan, [2] Department of Material Science and Engineering, University of Sheffield, Sheffield, United Kingdom, [3] Department of Physics, Abdul Wali Khan University, Mardan, Pakistan, [4] The Henry Royce Institute, Sheffield, United Kingdom, [5] Chemistry Department, King Saud University, Riyadh, Saudi Arabia, [6] School of Materials and Mineral Resources Engineering, Universiti Sains Malaysia, Nibong Tebal, Malaysia, [7] Electronic Materials Research Laboratory, Key Laboratory of the Ministry of Education & International Center for Dielectric Research, Xi'an Jiaotong University, Xi'an, China

OPEN ACCESS

Edited by:
Laijun Liu,
Guilin University of Technology, China

Reviewed by:
Zhuo Li,
Chang'an University, China
Haibo Yang,
Shaanxi University of Science and Technology, China
Yong Li,
Inner Mongolia University of Science and Technology, China

***Correspondence:**
Fayaz Hussain
fhussain@neduet.edu.pk;
engrfayazned@gmail.com
Di Zhou
zhoudi1220@xjtu.edu.cn

Specialty section:
This article was submitted to Ceramics and Glass, a section of the journal Frontiers in Materials

Received: 30 March 2020
Accepted: 04 May 2020
Published: 08 July 2020

Citation:
Hussain F, Khesro A, Lu Z, Alotaibi N, Mohamad AA, Wang G, Wang D and Zhou D (2020) Acceptor and Donor Dopants in Potassium Sodium Niobate Based Ceramics. Front. Mater. 7:160. doi: 10.3389/fmats.2020.00160

B-site doping in potassium sodium niobate (KNN) with Mn^{2+} (Mn'''_{Nb}) and Ti^{4+} (Ti'_{Nb}) dopants were soluble but prevented KNN from achieving a high relative density, while Sn^{4+} (Sn'_{Nb}) was not soluble in the structure as evidenced by second phase peaks in X-ray diffraction (XRD) traces. However, SnO_2 was an effective sintering aid in KNN-50/50. A-site doping with Sr^{2+} ($Sr^{\cdot}_{(Na,K)}$) up to 1 mol% initially improved dielectric properties but higher sintering temperatures were required for compositions with >1 mol% Sr. Samples with 5% and 7% of Sr-doping completely shifted the transition of T_{O-T} to below RT and broadened the T_C peaks as the relaxor. All Ti-doped and Sr-doped compositions showed an increase in conductivity, manifested as high values of dielectric loss (tanδ). More than 1% of acceptor and donor dopants showed the ionic-type conduction mechanism, while 1% displayed the electronic mechanism as attributed from the strongly frequency-dependent tanδ. In conclusion, these samples have the potential to open up new applications in the field of electroceramics.

Keywords: acceptor doping, donor doping, solubility, KNN, dielectric properties

INTRODUCTION

Different properties and effects of dopants on potassium sodium niobate (KNN)-based ceramics have been discussed in many publications (Lin et al., 2007; Lee et al., 2008; Wang et al., 2008; Liu et al., 2009, 2012; Tan et al., 2012; Zhao et al., 2013; Bafandeh et al., 2014; Wu J. et al., 2014; Zheng et al., 2015; Yang et al., 2016; Hussain et al., 2019, 2020). Some groups have discussed potassium oxide and sodium oxide both separately and with doping elements, in terms of electrical properties for KNN-based ceramics (Jaffe et al., 1971; Fluckiger and Arend, 1978; Kodaira et al., 1982; Jenko et al., 2005; Lee et al., 2008; Wang et al., 2008; Zhang et al., 2013; Zhao et al., 2013; Zheng et al., 2015). Fewer studies have been done on acceptor (Akça and Yılmaz, 2015; Rafiq et al., 2015; Chen et al., 2016) and donor (Wu S. et al., 2014; Hreščak et al., 2017) dopants in KNN to understand its electrical properties. Donor and acceptor dopants play a vital role in the investigation into the semiconducting properties and defect chemistry of the well-established systems of Barium Titanate (BT) and Lead Zirconate

Titanate (PZT; Masó et al., 2006; Da-Wei et al., 2009; Cao et al., 2010; Erdem et al., 2010; Wang D. W. et al., 2011; Wang et al., 2012, 2014; Wang D. et al., 2013; Ma et al., 2012; Zhu et al., 2012; Ali et al., 2013; Freeman et al., 2013; Li et al., 2013, 2015; Lou et al., 2018). Hreščak et al. (2017) reported Sr^{2+} as a donor dopant in KNN that improved its crystal structure, grain size, and phase composition. Rafiq et al. (2015) reported that the single acceptor-dopant of Mn^{2+} in KNN decreased the leakage current; most authors, however, have emphasized the importance of co-doping (Guo et al., 2004, 2005; Hollenstein et al., 2005; Hollenstein et al., 2007; Jiang et al., 2007; Lopez-Juarez et al., 2011; Rubio-Marcos et al., 2011; Skidmore and Milne, 2011; Wang H. Q. et al., 2011; Wang K. et al., 2013; Wang et al., 2017; Zhang et al., 2011; Li et al.,

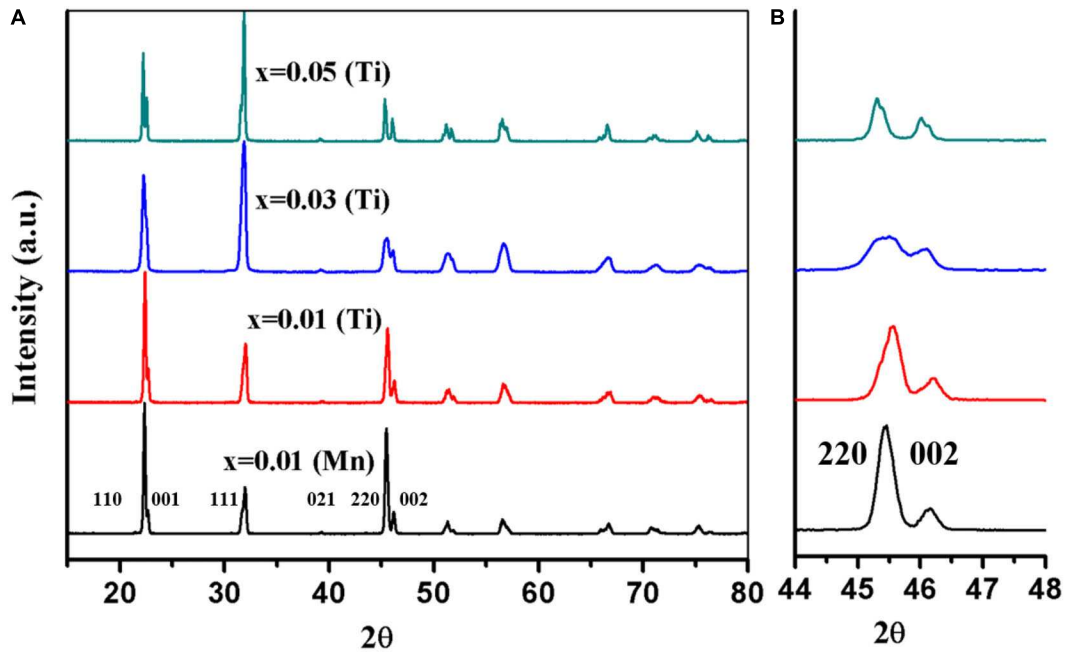

FIGURE 1 | (A) Single phase XRD patterns of Mn- and Ti-doped KNN-50/50, **(B)** zoomed peaks at 2θ ~ 45–46.

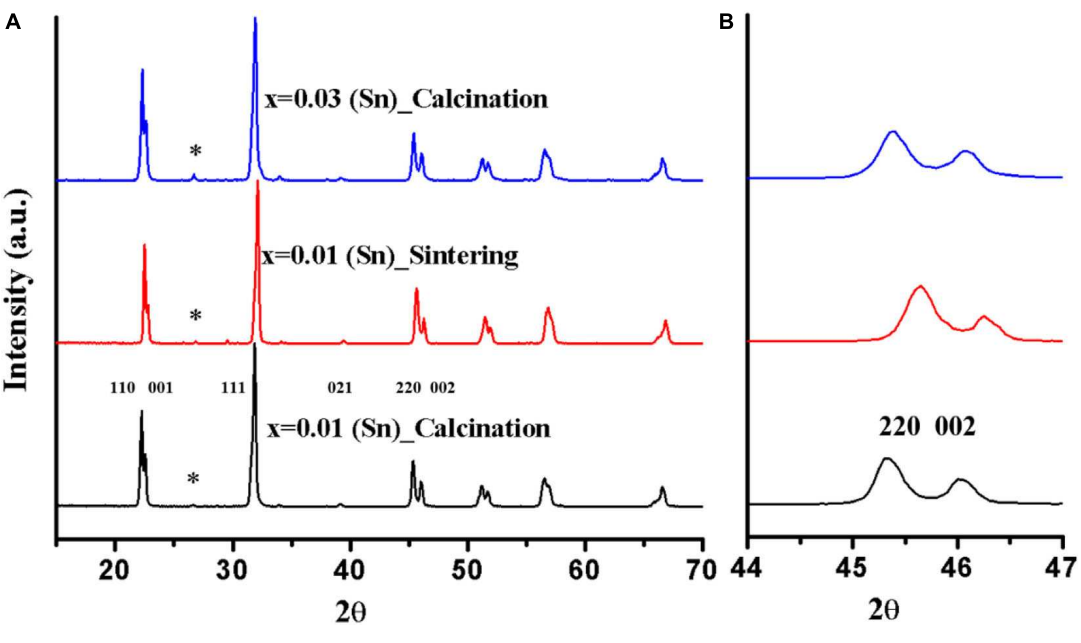

FIGURE 2 | (A) XRD patterns of Sn-doped KNN-50/50, **(B)** zoomed peak at 2θ ~ 45–46.

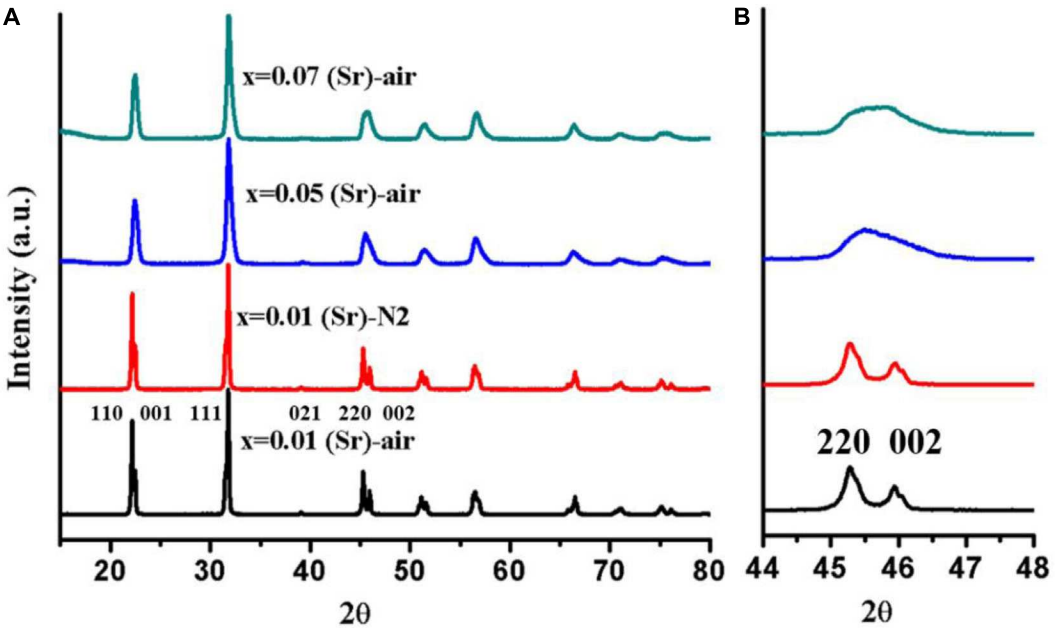

FIGURE 3 | (A) X-ray diffraction data of Sr doped KNN-50/50, **(B)** zoomed peak at 2θ ∼ 45–46.

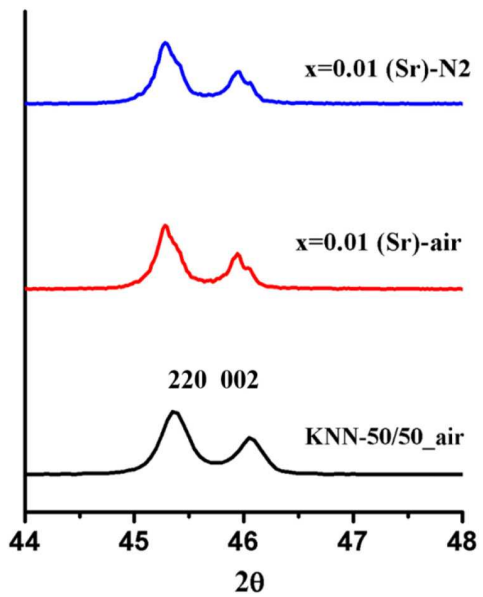

FIGURE 4 | Zoomed peak at 2θ ∼ 45–46, in comparision with the peak shape of 1% Sr_air/N_2 with KNN_50/50_air.

2012; Du et al., 2012a,b; Gio and Phong, 2015; Liu et al., 2016, 2017) in achieving optimized functional properties. Chen et al. (2016) prepared different formulations with trace amounts of acceptor-dopants into $(K_{0.5}Na_{0.5}\ Nb_{0.994}A_{0.006})O_{3-\delta}$, where A($Ga^{3+}$, Ge^{4+}, Mn^{2+}, Zn^{2+}, Cu^{2+}, and Ni^{2+}) metallic-ions were incorporated; this consequently improved the high mechanical-quality-factor (Q_m) values in divalent-doped compositions.

The aim of this research was to introduce acceptor-dopants (Mn^{2+}, Ti^{4+}, and Sn^{4+}) and donor-dopants (Sr^{2+}) into KNN to see the individual effect of their solubility and structural changes on the electrical properties of KNN-50/50-based ceramics.

EXPERIMENTAL PROCEDURE

Nb_2O_5 was obtained from Stanford Materials Corporation with 99.999% purity, whereas K_2CO_3 and Na_2CO_3 were obtained from Fisher Scientific with 99.9% anhydrous used. In addition to this, TiO_2 was obtained from Aldrich Chemistry with 99.99%, and MnO_2, SnO_2, and $SrCO_3$ were obtained from Aldrich with 99.9% purity each. Carbonates were dried at 300°C, whereas all other oxides were heated at 900°C for 24 h. Batches of 50 *g* of doped-KNN formulations ($K_{0.5}Na_{0.5}Ti_xNb_{1-x}O_{3-x/2}$ where $0.0 \leq x \leq 0.05$; $K_{0.5}Na_{0.5}Mn_xNb_{1-x}O_{3-x/2}$ where $0.0 \leq x \leq 0.01$; $K_{0.5}Na_{0.5}Sn_xNb_{1-x}O_{3-x/2}$ where $0.0 \leq x \leq 0.03$; and $(K_{0.5}Na_{0.5})_{1-x}Sr_xNbO_3$ where $0.0 \leq x \leq 0.07$) were prepared from dried raw powders in a hot condition (∼200°C) to avoid the non-stoichiometric conditions caused by moisture, especially in carbonates. All compositions were attrition milled for 1 h in a 500 ml jar at 300 rpm in isopropanol using 3 mm Dia. Y_2O_3 stabilized zirconia milling media prior to calcination. After milling, the slurry was washed with further isopropanol, separated from milling media through a sieve, and volatiles were removed at 80°C for 24 h in a drying oven. The dried material was sieved through a 150-micron mesh and calcined for 6 h at 850°C at 3°C/min and 5°C/min, heating and cooling rates, respectively. Reacted powders were re-milled before pressing a pellet. 10 mm diameter disks of all compounds were pressed uniaxially with 2-ton force and fired at in a temperature range of 1120–1165°C

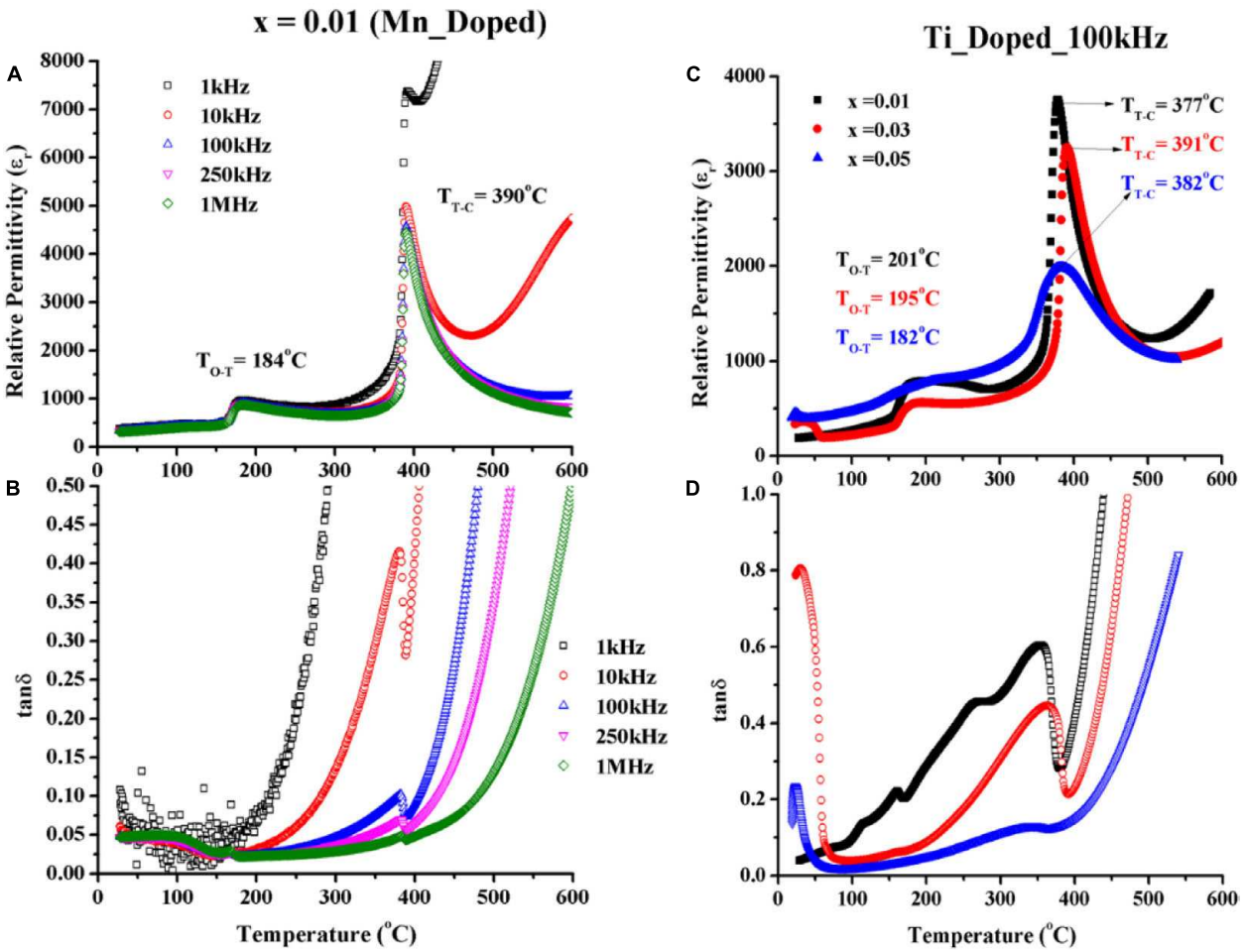

FIGURE 5 | (A) ε_r and **(B)** tanδ versus temperature of Mn-doped KNN; **(C)** ε_r and **(D)** tanδ versus temperature of Ti-doped KNN compositions.

for 2–8 h. Moreover, the details of sintering temperatures of all formulations are described in **Supplementary Figures S1, S2**.

Densities of pellets were measured as per the Archimedes method, which were around 90%-bulk in average. XRD traces of sintered pellets were obtained using a Siemens D500 diffractometer at the 2θ range of 10^o–80^o, using CuKα radiation. The dielectric properties were characterised using an LCR meter (Model 4284A, Hewlett Packard).

RESULTS AND DISCUSSION

XRD

The XRD traces from KNN-50/50 doped on the B-site with Mn^{2+}, Ti^{4+}, and Sn^{4+} are shown in **Figures 1**, **2**. The XRD traces from KNN-50/50 doped with 1% Mn and 1% Ti both appear to be similar, but the shape of 2θ ∼ 45° {220}, and {002} peaks shows a slight difference (**Figure 1**). In both cases, the intensity of the 2θ = 32° {111} is lower than that of the undoped KNN (Lin et al., 2010). Increasing the concentration of Ti to 5% Ti emphasized the structural change observed at 1% Ti. There are a few studies on single Mn acceptor dopant in KNN. Peaks shifting toward higher 2θ is evidence of shrinkage in the lattice volume, which took place for Mn^{2+} (Rafiq et al., 2015) and Ti^{4+} acceptor dopants as compared to the undoped KNN peak (shown in **Figure 4**; 2θ = 45–46°). Conversely, Lin et al. (2010) reported that XRD peaks shifted toward lower 2θ (i.e., expansion in the lattice volume) in the case of Mn^{4+} doped KNN.

For KNN-50/50 doped with Sn^{4+}, secondary peaks of SnO_2 are visible in **Figure 2**. Moreover, within the resolution limits of in-house XRD, there was no discernible change in the trace of the major KNN peaks, confirming that Sn does not enter into solid solution with KNN. Su et al. (2010) investigated SnO_2 and CuO co-doping in KNN and concluded that Sn^{4+} was not soluble after 1 mol%. Their XRD traces also depicted secondary peak positions similar to those in this study. Akça and Yılmaz (2015) also reported insolubility issues for Sn^{4+} in KNN with secondary peaks visible in their XRD data. The reasons behind the insolubility of Sn^{4+} issues in KNN is unclear, since Sn^{4+} (0.69 Å) has a similar ionic radius to Nb^{5+} (0.68 Å; Shannon, 1976). However, Sn^{4+} is more covalently bonded to O than Nb^{5+}, which may influence its solubility (Barret, 1962; IBchem, 2016).

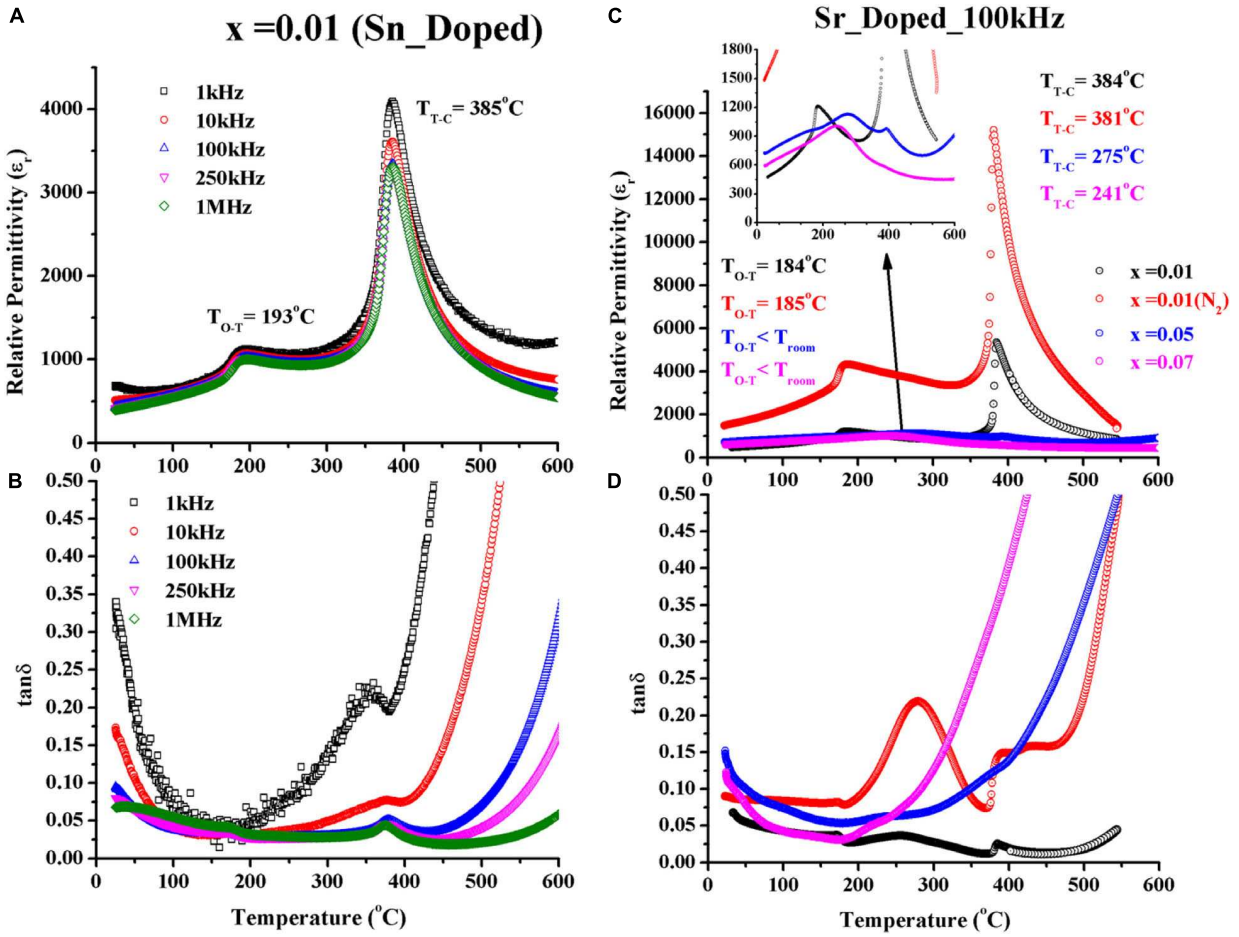

FIGURE 6 | (A) ε_r and **(B)** tanδ verses temperature of Sn-doped KNN; **(C)** ε_r and **(D)** tanδ verses temperature of Sr-doped KNN compositions.

For KNN-50/50 doped with Sr^{2+} on the A-site, the XRD traces revealed a broadening of the {111} peaks as a function of x with respect to undoped KNN-50/50 when fired in both air and N_2. **Figures 3**, **4** should be evaluated together, indicating that Sr^{2+} was incorporated within the KNN lattice.

Dielectric Properties

Acceptor Dopants: Mn^{2+}, Ti^{4+}, and Sn^{4+}

The temperature dependence of relative permittivity (ε_r) and loss (tanδ) of 1 mol% Mn doped KNN-50/50 are shown in **Figures 5A,B** as a function of temperature and frequency. Two phase transition temperatures, i.e., orthorhombic-tetragonal (T_{O-T}), and tetragonal-cubic (T_{T-C}) are clearly presented, though both transitions are shifted toward lower temperatures compared to undoped KNN-50/50 sintered in air. The ε_r and tanδ at room temperature of 1% Mn doped KNN-50/50 was 380 and 0.05 at 100 kHz, respectively. However, at lower frequencies, the tanδ increased dramatically when increasing the temperature. The most likely cause of tanδ relates to oxygen vacancy ($V_O^{\cdot\cdot}$) formed according to the defect equation:

$$Mn_{Nb}''' \equiv 3/2V_O^{\bullet\bullet}$$

At high frequencies (1 MHz), tanδ was suppressed with acceptor Mn^{2+} dopant. At these frequencies, the loss mechanism relating to $V_O^{\cdot\cdot}$ may clamp out, resulting in a decrease in the overall tanδ. There are a number of potential loss mechanisms relating to $V_O^{\cdot\cdot}$, such as rotation of defect dipoles and movement of space charge. It is not known which mechanism dominates in this study.

The dielectric properties of Ti-doped KNN-50/50 are shown in **Figures 5C,D**. For low concentrations, (1%) the T_{T-C} temperature decreased with little change in T_{O-T}. However, for high concentrations, T_{T-C} phase transition temperatures increased, and T_{O-T} decreased compared to the undoped and 1% Ti doped compositions and the phase transitions become broader. The peak in permittivity at around room temperature in 3 and 5% Ti-doped KNN may relate to the observation of minor changes to the shape of some XRD peaks (at {220} and {002} planes; **Figure 1**). Dielectric loss in Ti-doped suppressed from $x = 0.01$ to $x = 0.05$ with respect to the temperature and frequency, which suggested that the conduction mechanism shifted from electronic to ionic as the Ti dopant increased. Nevertheless, electronic species are lighter than ionic ones; that's why ionic species need more activation energy and consequently higher conductions at higher temperatures (see **Supplementary Data**).

The dielectric properties of Sn^{4+} doped KNN are shown in **Figures 6A,B**. Unsurprisingly, there was no effect on the dielectric properties with respect to undoped compositions since there was no evidence that Sn^{4+} enters the KNN lattice.

Donor Dopant: Sr^{2+}

Dielectric properties of Sr donor dopant (A-site) in KNN-50/50 are presented in **Figures 6C,D**. 1% Sr-doped KNN-50/50 compositions were sintered in both air and N_2 to compare the behavior with undoped in a previous study (Hussain et al., 2018) and acceptor doped compositions in the previous sections. However, for undoped KNN sintered in N_2, the transition temperature decreased in agreement with 1% Sr-doped KNN (N_2). N_2 sintered Sr^{2+} KNN becomes more conductive as compared to undoped KNN, presumably because Sr^{2+} donates extra electrons ($h^{\cdot}$) and low pO_2 creates $V_O^{\cdot\cdot}$. It has been proposed that the increase in conductivity contributes to the larger permittivity for N_2 sintered KNN-1 Sr. T_{T-C} with acceptor (Mn^{2+}) and donor (Sr^{2+}) in air are 390°C and 384°C, respectively, which suggests that disruption of the ferroelectric order to reduce T_{T-C} is greater for A-site Sr^{2+} doping in comparison to B-site Mn^{2+}. At higher Sr concentrations, $x = 0.05$ and 0.07, the phase transitions broaden in temperature (inset of **Figure 6C**), consistent with the broadening of peaks in the XRD traces (**Figure 3**). In addition, the dielectric loss increased when samples became more conductive at higher than 1% Sr (see **Supplementary Data**). Nonetheless, this broadening and higher dielectric loss phenomenon with donor doping looks similar to the results reported in the case of W^{6+} B-site donor doping in KNN, investigated by Wu S. et al. (2014).

CONCLUSION

Acceptor dopants such as Mn^{2+} (Mn_{Nb}''') and Ti^{4+} (Ti_{Nb}') at the B-site of KNN were incorporated to modify properties, but they both inhibited densification of KNN. Nonetheless, both acceptor species were soluble in the lattice, as revealed by XRD. Dielectric losses increased dramatically at lower frequencies with increasing temperatures by using acceptors but were moderately lower at higher frequencies. A further B-site dopant (Sn^{4+}) was also attempted but was insoluble, as evidenced by the appearance of secondary phase peaks in XRD data at low concentrations. Nevertheless, Sn^{4+} was an effective sintering aid in KNN-50/50 and improved its relative density. Ceramic density improved with 1 mol% Sr^{2+} but at a higher sintering temperature. Sr^{2+}-doped formulations showed higher conductivity, which manifested itself in higher values of tanδ. T_C of KNN-1 Sr in N_2 decreased with respect to air-sintered samples.

DATA AVAILABILITY STATEMENT

The raw data supporting the conclusions of this article will be made available by the authors, without undue reservation.

AUTHOR CONTRIBUTIONS

FH: Investigation, software, data analysis, original draft writing, and critical discussion of results, etc. AK: Formal discussion, review and editing, and language. ZL: Conceptualization, review, and editing. NA, GW, and DZ: Review, editing, and technical additions. AM: Review, editing, and technical discussion. DW: Review, editing, formal analysis, and critical discussion. All authors contributed to the article and approved the submitted version.

FUNDING

FH acknowledges NED University of Engineering and Technology, Pakistan, for funding support. All authors acknowledge financial help from the Sustainability and Substitution of Functional Materials and Devices EPSRC grant (EP/L017563/1) through Prof. Ian M. Reaney. The data of this work is from Ph.D. thesis of FH (Corresponding Author; Hussain, 2016). ZL acknowledges the Henry Royce Institute for Advanced Materials, funded through EPSRC grants EP/R00661X/1, EP/S019367/1, EP/P02470X/1, and EP/P025285/1.

SUPPLEMENTARY MATERIAL

The Supplementary Material for this article can be found online at: https://www.frontiersin.org/articles/10.3389/fmats.2020.00160/full#supplementary-material

REFERENCES

Akça, E., and Yılmaz, H. (2015). Sintering behavior and electrical properties of K4CuNb8O23 modified K0.5Na0.5NbO3 ceramics with SnO2, ZnO or Yb2O3 doping. *Ceramics Int.* 41, 3659–3667. doi: 10.1016/j.ceramint.2014.11.035

Ali, A. I., Ahn, C. W., and Kim, Y. S. (2013). Enhancement of piezoelectric and ferroelectric properties of BaTiO 3 ceramics by aluminum doping. *Ceramics Int.* 39, 6623–6629. doi: 10.1016/j.ceramint.2013.01.099

Bafandeh, M. R., Gharahkhani, R., Abbasi, M. H., Saidi, A., Lee, J.-S., and Han, H.-S. (2014). Improvement of piezoelectric and ferroelectric properties in (K,Na)NbO3- based ceramics via microwave sintering. *J. Electr.* 33, 128–133. doi: 10.1007/s10832-014-9951-z

Barret, R. L. (1962). Electronegativity Chart. *J. Chem. Educ.* 39:251. doi: 10.1021/ed039p251

Cao, M.-S., Wang, D.-W., Yuan, J., Lin, H.-B., Zhao, Q.-L., Song, W.-L., et al. (2010). Enhanced piezoelectric and mechanical properties of ZnO whiskers and Sb2O3 co-modified lead zirconate titanate composites. *Mater. Lett.* 64, 1798–1801. doi: 10.1016/j.matlet.2010.05.037

Chen, K., Zhang, F., Li, D., Tang, J., Jiao, Y., and An, L. (2016). Acceptor doping effects in (K0.5Na0.5)NbO3 lead-free piezoelectric ceramics. *Ceramics Int.* 42, 2899–2903. doi: 10.1016/j.ceramint.2015.11.016

Da-Wei, W., De-Qing, Z., Jie, Y., Quan-Liang, Z., Hong-Mei, L., Zhi-Ying, W., et al. (2009). Structural and electrical properties of Nd ion modified lead zirconate titanate nanopowders and ceramics. *Chin. Phys. B* 18:2596. doi: 10.1088/1674-1056/18/6/079

Du, J., Yi, X.-J., Ban, C.-L., Xu, Z.-J., Zhao, P.-P., and Wang, C.-M. (2012a). Piezoelectric properties and time stability of lead-free (Na0.52K0.44Li0.04)Nb1-x-ySbxTayO3 ceramics. *Ceramics Int.* 39, 2135–2139. doi: 10.1016/j.ceramint.2012.07.063

Du, J., Yi, X.-J., Xu, Z.-J., Ban, C.-L., Zhang, D.-F., Zhao, P.-P., et al. (2012b). Effects of CaAl2O4 on the electrical properties and temperature stability of (Na0.53K0.404Li0.066)Nb0.92Sb0.08O3 ceramics. *J. Alloys Compounds* 541, 454–457. doi: 10.1016/j.jallcom.2012.07.039

Erdem, E., Eichel, R. A., and Fetzer, C., Dézsi, I., Lauterbach, S., Kleebe, H. J., et al. (2010). Site of incorporation and solubility for Fe ions in acceptor-doped PZT ceramics. *Journal of Applied Physics* 107, 054109. doi: 10.1063/1.3327436

Hussain, F. (2016). *Lead-Free KNN-based Piezoelectric Ceramics*. PhD thesis, The University of Sheffield, United Kingdom.

Fluckiger, U. and Arend, H. (1978). On the preparation of pure, doped and reduced $KNBO_3$ single crystals. *J. Crystal Growth* 43, 406–416. doi: 10.1016/0022-0248(78)90338-x

Freeman, C. L., Dawson, J. A., Chen, H.-R., Ben, L., Harding, J. H., Morrison, F. D., et al. (2013). Energetics of Donor-Doping, Metal Vacancies, and Oxygen-Loss in A-Site Rare-Earth-Doped BaTiO3. *Adv. Funct. Mater.* 23, 3925–3928. doi: 10.1002/adfm.201203147

Gio, P. D., and Phong, N. D. (2015). Effects of LiF on the Structure and Electrical Properties of $(Na_{0.52}\ K_{0.435}\ Li_{0.045})\ Nb_{0.87}\ Sb_{0.08}\ Ta_{0.05}\ O_3$ Lead-Free Piezoelectric Ceramics Sintered at Low Temperatures. *J. Mater. Sci. Chem. Eng.* 03, 13–20. doi: 10.4236/msce.2015.311003

Guo, Y., Kakimoto, K. I., and Ohsato, H. (2004). Phase transitional behavior and piezoelectric properties of (Na[sub 0.5]K[sub 0.5])NbO[sub 3]–LiNbO[sub 3] ceramics. *Appl. Phys. Lett.* 85:4121.

Guo, Y., Kakimoto, K. I., and Ohsato, H. (2005). (Na0.5K0.5)NbO3–LiTaO3 lead-free piezoelectric ceramics. *Mater. Lett.* 59, 241–244. doi: 10.1016/j.matlet.2004.07.057

Hollenstein, E., Damjanovic, D., and Setter, N. (2007). Temperature stability of the piezoelectric properties of Li-modified KNN ceramics. *J. Eur. Ceramic Soc.* 27, 4093–4097. doi: 10.1016/j.jeurceramsoc.2007.02.100

Hollenstein, E., Davis, M., Damjanovic, D., and Setter, N. (2005). Piezoelectric properties of Li- and Ta-modified (K[sub 0.5]Na[sub 0.5])NbO[sub 3] ceramics. *Appl. Phys. Lett.* 87:182905.

Hreščak, J., Dražić, G., Deluca, M., Arèon, I., Kodre, A., Dapiaggi, M., et al. (2017). Donor doping of K 0.5 Na 0.5 NbO 3 ceramics with strontium and its implications to grain size, phase composition and crystal structure. *J. Eur. Ceramic Soc.* 37, 2073–2082. doi: 10.1016/j.jeurceramsoc.2016.12.053

Hussain, F., Sterianou, I., Khesro, A., Sinclair, D. C., and Reaney, I. (2018). p-Type/n-type behaviour and functional properties of $K_xNa_{(1-x)}\ NbO_3$ (0.49= x= 0.51) sintered in air and N_2. *J. Eur. Ceramic Soc.* 38, 3118–3126. doi: 10.1016/j.jeurceramsoc.2018.03.013

Hussain, F., Khesro, A., Lu, Z., Wang, G., and Wang, D. (2020). Lead free multilayer piezoelectric actuators by economically new approach. *Front. Mater.* 7:87. doi: 10.3389/fmats.2020.00087

Hussain, F., Khesro, A., Muhammad, R., and Wang, D. (2019). Effect of Ta-doping on functional properties of K0.51Na0.49NbO3. *Mater. Res. Expr.* 6:106309. doi: 10.1088/2053-1591/ab3d49

IBchem (2016). *Covalent Bond*. Brussels: IBchem.

Jaffe, B., Cook, W. R. J., and Jaffe, H. (1971). *Piezoelectric Ceramics*. New York, NY: Academic Press.

Jenko, D., Bencan, A., Malic, B., Holc, J., and Kosec, M. (2005). Electron microscopy studies of potassium sodium niobate ceramics. *Microsc Microanal* 11, 572–580. doi: 10.1017/s1431927605050683

Jiang, X. P., Hu, X. P., Jiang, F. L., Liu, X. D., and Yin, Q. R. (2007). Li-modified sodium potassium tantalum niobate lead-free piezoelectric ceramics. *J. Inorgan. Mater.* 22, 465–468.

Kodaira, K., Shioya, J., Shimada, S., Matsushita, T. (1982). Sintering and dielectric properties of $KNbO_3$. *J. Mater. Sci. Lett.* 1, 277–278.

Lee, Y.-H., Cho, J.-H., Kim, B.-I., and Choi, D.-K. (2008). Piezoelectric Properties and Densification Based on Control of Volatile Mass of Potassium and Sodium in (K0.5Na0.5)NbO3Ceramics. *Jpn. J. Appl. Phys.* 47, 4620–4622. doi: 10.1143/jjap.47.4620

Li, Y., Dai, Y.-J., Wang, H.-Q., Sun, T., Xu, W., and Zhang, X.-W. (2012). Microstructures and electrical properties of KNbO3 doped (Li,Ta,Sb) modified (K,Na)NbO3 lead-free ceramics by two-step sintering. *Mater. Lett.* 89, 70–73. doi: 10.1016/j.matlet.2012.08.061

Li, Y., Wang, D., Cao, W., Li, B., Yuan, J., Zhang, D., et al. (2015). Effect of MnO2 addition on relaxor behavior and electrical properties of PMNST ferroelectric ceramics. *Ceramics Int.* 41, 9647–9654. doi: 10.1016/j.ceramint.2015.04.030

Li, Y., Yuan, J., Wang, D., Zhang, D., Jin, H., and Cao, M. (2013). Effects of Nb, Mn doping on the structure, piezoelectric, and dielectric Properties of 0.8 Pb (Sn 0.46 Ti 0.54) O 3–0.2 Pb (Mg 1/3 Nb 2/3) O 3 piezoelectric ceramics. *J. Am. Ceramic Soc.* 96, 3440–3447.

Lin, D., Li, Z., Zhang, S., Xu, Z., Yao, X. (2010). Influence of MnO_2 doping on the dielectric and piezoelectric properties and domain structure in $(K_{0.5}Na_{0.5})NbO_3$ single crystals. *J. Am. Ceramic Soc.* 93, 941–944.

Lin, D., Kwok, K. W., and Chan, H. W. L. (2007). Dielectric and piezoelectric properties of $(K_{0.50}Na_{0.50}NbO_3–BaZr_{0.050}Ti_{0.950}O_3)$ lead-free ceramics. *Appl. Phys. Lett.* 91:143513.

Liu, L., Fan, H., Fang, L., Chen, X., Dammak, H., and Thi, M. P. (2009). Effects of Na/K evaporation on electrical properties and intrinsic defects in Na0. 5K0. 5NbO3 ceramics. *Mater. Chem. Phys.* 117, 138–141. doi: 10.1016/j.matchemphys.2009.05.024

Liu, L., Huang, Y., Li, Y., Fang, L., Dammak, H., Fan, H., et al. (2012). Orthorhombic to tetragonal structural phase transition in Na0. 5K0. 5NbO3-based ceramics. *Mater. Lett.* 68, 300–302. doi: 10.1016/j.matlet.2011.10.103

Liu, L., Knapp, M., Ehrenberg, H., Fang, L., Fan, H., Schmitt, L. A., et al. (2017). Average vs. local structure and composition-property phase diagram of K0. 5Na0. 5NbO3-Bi$^1/_2$Na$^1/_2$TiO3 system. *J. Eur. Ceramic Soc.* 37, 1387–1399. doi: 10.1016/j.jeurceramsoc.2016.11.024

Liu, L., Knapp, M., Ehrenberg, H., Fang, L., Schmitt, L. A., Fuess, H., et al. (2016). The phase diagram of K0. 5Na0. 5NbO3–Bi1/2Na1/2TiO3. *J. Appl. Crystallogr.* 49, 574–584. doi: 10.1107/s1600576716002909

Lopez-Juarez, R., Gonzalez-Garcia, F., Zarate-Medina, J., Escalona-Gonzalez, R., and de la Torre, S. D., and Villafuerte-Castrejon, M. E. (2011). Piezoelectric properties of Li-Ta co-doped potassium-sodium niobate ceramics prepared by spark plasma and conventional sintering. *J. Alloys Compounds* 509, 3837–3842. doi: 10.1016/j.jallcom.2010.12.103

Lou, Q., Shi, X., Ruan, X., Zeng, J., Man, Z., Zheng, L., et al. (2018). Ferroelectric properties of Li-doped BaTiO3 ceramics. *J. Am. Ceramic Soc.* 101, 3597–3604.

Ma, N., Zhang, B.-P., and Yang, W.-G. (2012). Low-temperature sintering of Li2O-doped BaTiO3 lead-free piezoelectric ceramics. *J. Electroceram.* 28, 275–280. doi: 10.1007/s10832-012-9730-7

Masó, N., Beltrán, H., Cordoncillo, E., Flores, A. A., Escribano, P., Sinclair, D. C., et al. (2006). Synthesis and electrical properties of Nb-doped BaTiO3. *J. Mater. Chem.* 16, 3114–3119. doi: 10.1039/b601251e

Rafiq, M. A., Tkach, A., Costa, M. E., Vilarinho, P. M. (2015). Defects and charge transport in Mn-doped $K_{0.5}Na_{0.5}NbO_3$ ceramics. *Phys. Chem. Chem. Phys.* 17, 24403–24411. doi: 10.1039/c5cp02883c

Rubio-Marcos, F., Romero, J. J., Fernández, J. F., and Marchet, P. (2011). Control of the Crystalline Structure and Piezoelectric Properties of (K,Na,Li)(Nb,Ta,Sb)O$_{3}$ Ceramics through Transition Metal Oxide Doping. *Appl. Phys. Expr.* 4:101501. doi: 10.1143/apex.4.101501

Shannon, R. D. (1976). Revised effective ionic radii and systematic studies of interatomie distances in halides and chalcogenides. *Acta Crystallogr. Sec. A* 32, 751–767. doi: 10.1107/s0567739476001551

Skidmore, T. A., and Milne, S. J. (2011). Phase development during mixed-oxide processing of a $[Na_{0.5}K_{0.5}NbO_3]_{1-x}–[LiTaO_3]_x$ powder. *J. Mater. Res.* 22, 2265–2272. doi: 10.1557/jmr.2007.0281

Su, S., Zuo, R., Wang, X., and Li, L. (2010). Sintering, microstructure and piezoelectric properties of CuO and SnO2 co-modified sodium potassium niobate ceramics. *Mater. Res. Bull.* 45, 124–128. doi: 10.1016/j.materresbull.2009.09.033

Tan, C. K. I., Yao, K., Goh, P. C., and Ma, J. (2012). 0.94(K0.5Na0.5)NbO3–0.06LiNbO3 piezoelectric ceramics prepared from the solid state reaction modified with polyvinylpyrrolidone (PVP) of different molecular weights. *Ceramics Int.* 38, 2513–2519. doi: 10.1016/j.ceramint.2011.11.021

Wang, D., Hussain, F., Khesro, A., Feteira, A., Tian, Y., Zhao, Q., et al. (2017). Composition and temperature dependence of structure and piezoelectricity

in (1- x)(K1- yNay) NbO3-x (Bi1/2Na1/2) ZrO3 lead-free ceramics. *J. Am. Ceramic Soc.* 100, 627–637. doi: 10.1111/jace.14589

Wang, D., Li, J., Cao, M., and Zhang, S. (2014). Effects of Nb 2 O 5 additive on the piezoelectric and dielectric properties of PHT-PMN ternary ceramics near the morphotropic phase boundary. *Phys. Status Solidi. A Appl. Mater. Sci.* 211, 226–230. doi: 10.1002/pssa.201330203

Wang, D., Zhao, Q., Cao, M., Cui, Y., and Zhang, S. (2013). Dielectric, piezoelectric, and ferroelectric properties of Al2O3 and Mn O 2 modified Pb S n O 3–P b T i O 3–P b (M g1/3Nb2/3) O 3 ternary ceramics. *Phys. Status Solidi* 210, 1363–1368. doi: 10.1002/pssa.201228760

Wang, D. W., Cao, M. S., Yuan, J., Zhao, Q. L., Li, H. B., Zhang, D. Q., et al. (2011). Enhanced Piezoelectric and Ferroelectric Properties of Nb2O5 Modified Lead Zirconate Titanate-Based Composites. *J. Am. Ceramic Soc.* 94, 647–650. doi: 10.1111/j.1551-2916.2010.04309.x

Wang, D.-W., Yuan, J., Li, H.-B., Lu, R., Zhao, Q.-L., Zhang, D.-Q., et al. (2012). Effects of Nb 2 O 5 addition on the microstructure, electrical, and mechanical properties of PZT/ZnO nanowhisker piezoelectric composites. *J. Mater. Sci.* 47, 2687–2694. doi: 10.1007/s10853-011-6094-3

Wang, H. Q., Zuo, R. Z., Fu, J. A., and Liu, Y. (2011). Sol-gel derived (Li, Ta, Sb) modified sodium potassium niobate ceramics: processing and piezoelectric properties. *J. Alloys Compounds* 509, 936–941. doi: 10.1016/j.jallcom.2010.09.134

Wang, K., Yao, F.-Z., Jo, W., Gobeljic, D., Shvartsman, V. V., Lupascu, D. C., et al. (2013). Temperature-Insensitive (K,Na)NbO3-Based Lead-Free Piezoactuator Ceramics. *Adv. Funct. Mater.* 23, 4079–4086. doi: 10.1002/adfm.201203754

Wang, Y., Damjanovic, D., Klein, N., and Setter, N. (2008). High-Temperature Instability of Li- and Ta-Modified (K,Na)NbO3Piezoceramics. *J. Am. Ceramic Soc.* 91, 1962–1970. doi: 10.1111/j.1551-2916.2008.02392.x

Wu, J., Wang, X., Cheng, X., Zheng, T., Zhang, B., Xiao, D., et al. (2014). New potassium-sodium niobate lead-free piezoceramic: Giant-d33 vs. sintering temperature. *J. Appl. Phys.* 115:114104. doi: 10.1063/1.4868585

Wu, S., Zhu, W., Liu, L., Shi, D., Zheng, S., Huang, Y., et al. (2014). Dielectric properties and defect chemistry of WO 3-doped K 0.5 Na 0.5 NbO 3 ceramics. *J. Electr. Mater.* 43, 1055–1061.

Yang, X., Cheng, Z., Cheng, J., Wang, D., Shi, F., Zheng, G., et al. (2016). Structural and ferroelectric properties of textured KNN thick films prepared by sol-gel methods. *Integr. Ferroelectr.* 176, 171–178. doi: 10.1080/10584587.2016.1252242

Zhang, D.-Q., Wang, D.-W., Zhu, H.-B., Yang, X.-Y., Lu, R., Wen, B., et al. (2013). Synthesis and characterization of single-crystalline (K, Na) NbO3 nanorods. *Ceramics Int.* 39, 5931–5935. doi: 10.1016/j.ceramint.2012.11.065

Zhang, L., Shen, J., Yu, J., Zhao, H., Xiu, Z., Yan, C., et al. (2011). Normal sintering and electric properties of (K,Na,Li)(Nb,Sb)O3 lead-free piezoelectric ceramics. *J. Electroceram.* 26, 105–111. doi: 10.1007/s10832-011-9636-9

Zhao, Y., Huang, R., Liu, R., Zhou, H., and Zhao, W. (2013). Low-temperature sintering of KNN with excess alkaline elements and the study of its ferroelectric domain structure. *Curr. Appl. Phys.* 13, 2082–2086. doi: 10.1016/j.cap.2013.08.015

Zheng, T., Wu, J., Xiao, D., and Zhu, J. (2015). Giant d33 in nonstoichiometric (K,Na)NbO3-based lead-free ceramics. *Script. Mater.* 94, 25–27. doi: 10.1016/j.scriptamat.2014.09.008

Zhu, W., Fujii, I., Ren, W., Trolier-McKinstry, S., and Jones, J. (2012). Domain Wall Motion in A and B Site Donor-Doped Pb(Zr0.52Ti0.48)O3 Films. *J. Am. Ceramic Soc.* 95, 2906–2913. doi: 10.1111/j.1551-2916.2012.05243.x

Conflict of Interest: The authors declare that the research was conducted in the absence of any commercial or financial relationships that could be construed as a potential conflict of interest.